The Journal of Physical Chemistry A

 VOLUME 102, NUMBER 49, DECEMBER 3, 1998

ARTICLES

Electrostatic Insights into the Molecular Hydration Process: A Case Study of Crown Ethers†

Subhash S. Pingale and Shridhar R. Gadre*

Department of Chemistry, University of Pune, Pune 411 007, India

Libero J. Bartolotti

North Carolina Supercomputing Center, 3021 Cornwallis Road, Research Triangle Park, North Carolina 27709

Received: June 2, 1998; In Final Form: August 28, 1998

Ab initio quantum chemical methods as well as simulation/dynamics programs have been conventionally used for probing the hydration of molecules, an important problem in chemistry and biology. However, very few attempts have as yet been reported for *understanding the stepwise patterns* in hydration processes at the molecular level. The present work investigates the problem of hydration of the 18-crown-6 (18C6) molecule based on rigorous topography mapping of molecular electrostatic potential (MESP) followed by an application of a simple electrostatic model (electrostatic potential for intermolecular complexation) for obtaining trends in energetics. Structures and energies of the hydrated species, 18C6·nH$_2$O (n = 1, 2, 3, 4, 6) have been studied by the EPIC model followed by ab initio HF/6-31G** investigations. The remarkable agreement between the model and ab initio results highlights the utility of MESP topography for exploring the lock-and-key features in a hydration process via cooperative electrostatic effects.

Introduction

The importance of the weak intermolecular bond, now called the hydrogen bond,[1] has been highlighted since the work of Latimer and Rodebush in 1920 on the structure and properties of water. In particular, the hydration[2] of molecules and ions constitutes a very important problem in a variety of chemical and biological systems. Several hydrates[3,4] have been subjected to X-ray diffraction studies for unearthing the hydrogen bond networks in their three-dimensional structures. Leszczynski et al.[5−8] have carried out many interesting ab initio level investigations for finding out the first hydration shell of chemically and biologically interesting molecules, as well as the stacked protonated base pairs.

The hydration problem has also been approached via molecular modeling methods in the literature. In earlier studies, Olivera[9] has studied binding of the water molecule to the component units of nucleic acids and B-DNA, with the help of an electrostatic model. In this method, energy calculations are implemented with overlap multiple procedure and the total interaction energy calculated between the two sets of multipoles, using the classical electrostatic expressions for the charge−charge, charge−dipole, charge−quadrupole, dipole−dipole, dipole−quadrupole, and quadrupole−quadrupole interactions. Recently, Orozco et al.[10] have proposed a methodology for computing a quantity christened by them as molecular interaction potential (MIP) for representing electrostatic interactions as well as steric effects in a combined way. The results obtained by them on nonbonded interactions demonstrated the superiority of MIP over the standard treatment using molecular electrostatic

† Dedicated to Professor Robert G. Parr on his 77th birthday.

10.1021/jp982444b CCC: $15.00
Published on Web 11/13/1998

potential (MESP). Alhambra et al.[11] have developed a new method for the representation of interaction between solutes and their hydration water based on generalization of the MIP with a parametrization of the van der Waals interactions between the solute and the water molecule. In this model, they have modified MIP to molecular solvation potential (MSP), which provides a better representation of noncovalent interactions between the molecule and dipole or higher order multipole. In MSP, Alhambra et al.[11] have optimized van der Waals parameters (which represent dispersion−repulsion interactions) with fitting MSP and ab initio 6-31G* data. Applications of MSP to hydration of several species, including DNA bases, were reported by them to be quite successful. Further, Alhambra et al.[11] have remarked that the specific polarization effect of water directly bound to the solute is not very large (i.e. nearly 7% to that of the total interaction energy) in MSP calculations. Luque et al.[12] have, however, found out later that the polarization energy in polar π-rich systems can be up to -2.0 kcal mol^{-1}, and such a contribution to the total free energy of solvation cannot be neglected.

Crown ether molecules has been employed as prototypes for such weak interaction studied in supramolecular chemistry. These macrocyclic polyethers have acquired importance in solution chemistry due to their action as effective carriers across membranes, as catalysts and as extracting agents in nonpolar media.[13] Further, from a fundamental point of view, the hydration of crown ethers has served as a classic example in supramolecular chemistry[14−18] with reference to host−guest interactions.

Hydration of crown ethers has been probed by a number of experimental techniques, viz. Raman spectroscopy,[17] infrared spectroscopy,[19] X-ray diffraction,[14,15,17e] quasielastic neutron scattering,[20] and ultrasonic spectroscopy.[21] Mootz et al.[14,15] have confirmed the existence of binary hydrates of 18-crown-6 (18C6) with the help of melting diagrams by the temperature-dependent X-ray powder diffraction method. They have investigated the crystal structures of crown ether hydrates, viz. of 18C6·nH$_2$O with $n = 4$, 6, 8, and 12, in which it has been found that the conformation of the 18C6 in the hydrate bears a symmetry close to a D_{3d} one. They have reported that these hydrates are formed with the hydrogen bond formed by oxygens of 18C6 and water with the hydrogen of water molecules. Matsuura et al.[17b] confirmed the formation of a crystalline complex between 18C6 and water with the help of the composition at the congruent melting point. The number of water molecules incorporated into an 18C6 moiety has been estimated by them to be approximately 4−6. They have also remarked that the determination of the exact stoichiometry of the complex is not possible. In a recent study on the 18C6···water system employing Raman spectroscopy in solid state, Fukuhara et al.[17a] have shown the formation of at least four distinct hydrates at liquid nitrogen temperature. They have noted the ratio of 18C6 to water for the two hydrates to be 1:6 and 1:4.5 with the D_{3d} conformation of the crown ring in these hydrates, which has also been confirmed by X-ray diffraction[17e] studies of aqueous solution. Bryan et al.[19] have investigated the interaction of water in carbon tetrachloride with the help of the Fourier transform infrared (FTIR) technique. In their study, they have probed H$_2$O bound to 18C6 in two different forms according to the number, position, and width of OH streching band of the complex 18C6 with H$_2$O in the ratio of 1:1. Out of these two, one water molecule is found to be attached to an ether oxygen atom by a single hydrogen bond and the other one involves a H$_2$O bridge with two ether oxygen atoms.

Crown ether hydrates also have been studied theoretically by molecular mechanics,[22] molecular dynamics,[23] and Monte Carlo calculations.[16,24] These studies bring out the centrosymmetric D_{3d} conformer to be the most stable one in aqueous solution. In a Monte Carlo simulation study, Ranghino et al.[16] have explored the hydration of 18C6 with a cluster made up of 100 water molecules surrounding the 18C6 in the C_i, D_{3d}, and C_1 conformations. It has been found that the intrinsically most stable C_i form is not so well-hydrated due to linear H bonds to the 18C6 and unfavorable water···water interactions. However, the D_{3d} form, with a suitably preformed cavity, is more stable than the C_1 form in water due to cooperativity of water molecules H bonded one to another. In this respect, Ranghino et al.[16] have posed a question: *Would it be possible to understand (or predict) at least trends in hydration process from simple consideration?* That the dipole moment of the solute cannot show the trends of solute−water interaction energy has been noted by Ranghino et al.[16] From the study of the molecular surface, they have observed that only for the D_{3d} conformer of 18C6, there is a cavity in the center of the ring, accessible to the solvent. With the analysis of the solvent-accessible surface and the potential energy surface, it is concluded that C_i conformation is less hydrated than the C_1 or D_{3d} ones because its hydrophilic binding sites are less exposed to the solvent. In a similar vein, Fukuhara et al.[17a] noted that a clear picture of hydration structure of the crown ether has not as yet emerged.

However, concerning the interaction of the crown ether with water, a neutral species, one may expect that electrostatic interactions will be dominant. MESP has been extensively used[25−31] for studying the weak molecular interactions, although the topographical aspect has not been much stressed.

In the current work, hydration patterns of 18C6 are investigated using MESP and a recently developed model by Gadre et al.,[30c] viz., electrostatic potential for intermolecular complexation (EPIC), based on MESP topography. This is followed by ab initio calculations to test out the validity of the present approach. The procedure employed for this study is discussed below.

Methodology

The geometries of 18C6 and H$_2$O monomers have been optimized at Hartree−Fock (HF) self-consistent field (SCF) level of ab initio theory using the 6-31G** basis set with the package GAUSSIAN.[32] The corresponding density matrix elements are utilized for the enumeration of MESP.[33]

The MESP, $V(r)$, at a point r in molecular framework with nuclear charges $\{Z_A\}$ located at $\{R_A\}$ and the corresponding electron density, $\rho(r)$, is given by

$$V(r) = \sum_A^N \frac{Z_A}{|R_A - r|} - \int \frac{\rho(r')}{|r' - r|} \mathrm{d}^3 r' \qquad (1)$$

where N is the total number of nuclei in the molecule. The two terms in the above equation represent the bare nuclear and electronic contributions, respectively. The sign of $V(r)$ at a given point represents whether the nuclear or electronic effects are dominant. Topographical[34] analysis of $V(r)$ is based on the location and characterization of the critical points (CPs), where the first-order partial derivatives of $V(r)$ vanishes. The CP is given a rank based on the number of nonzero eigenvalues of the Hessian matrix **A**, the elements of which are defined by

$$A_{ij} = \left.\frac{\partial^2 V(r)}{\partial x_i \, \partial x_j}\right|_{r=r_c} \qquad (2)$$

where r_c is a critical point. If all three eigenvalues of the Hessian matrix of $V(r)$ are nonzero, the CP may be further categorized into a (+3,+3), (+3,−3), (+3,+1) or (+3,−1) type, the second number in the parentheses denoting the sum of the signs of the Hessian matrix eigenvalues.[35] These topographical features of MESP are qualitatively exploited in the present work for predicting the potential H_2O binding sites of 18C6 and the orientation of H_2O molecules based on a *lock-and-key* mechanism. The MESP evaluation and topographical analysis are done using the package INDPROP[36] developed in our laboratory. As mentioned above, the EPIC[30c] model based on molecular electrostatic potential has been used for determination of structure and the energy of the complex. In this model, the interaction energy of the complex formed by molecules *A* and *B* is given by

$$E_{\text{int}} = \{\sum_i V_{A,i} q_{B,i} + \sum_j V_{B,j} q_{A,j}\}/2 \qquad (3)$$

where $V_{A,i}$ is the MESP value due to A at the *i*th atom of molecule B and $q_{B,i}$ is the potential derived atomic charge[35] (PD-AC) on the *i*th atom of B. The quantity E_{int} in eq 3 is minimized by a complete translation and rotation of molecule B with respect to A, to search for the minimum energy structure. The Pauling van der Waals radii[38] for atoms are employed generally for preventing the collapse of the two species. An appropriately scaled radius has, however, been chosen for the hydrogen[39] atom. The structure of 18C6·H_2O formed on the hydration of 18C6 by a single water molecule is optimized with the EPIC model and further utilized to find where the second H_2O molecule binds. Full ab initio SCF optimization of 18C6·H_2O has been done to check the reliability of model. For optimization of 18C6·$2H_2O$ with the EPIC model, 18C6·H_2O is treated as a monomer for docking with another H_2O molecule. The full SCF-optimized density matrix is used for carrying out topographical analysis of MESP and determining MESP-derived charges for 18C6·H_2O. In the present procedure, minimum parametrization is used for calculating model interaction energy as compared to the other models (e.g. those in refs 10−12). A similar procedure is employed for obtaining the binding energies and geometries of H_2O to 18C6·nH_2O, where $n = 2$ and 3. The graphical visualization of MESP isosurfaces and complex geometries has been carried out with the program UNIVIS.[40]

Results and Discussion

MESP topographical investigation of the 18C6 molecule bearing D_{3d} symmetry brings out six negative-valued (+3,+3) MESP minima that are present in the vicinity of each of the oxygens of 18C6. Figure 1 depicts six patches of negative-valued isosurfaces of value −288.8 kJ mol^{-1} each surrounding an MESP minimum of value −320.3 kJ mol^{-1}. Out of these, three minima are shifted slightly toward one of the faces of 18C6, and the other three, to the other one. The MESP minima of 18C6 are comparatively deeper in value than those of the H_2O molecule, viz., −261.2 kJ mol^{-1}. This negative MESP region may induce the first water (w_1) molecule to bind to 18C6 by forming hydrogen bonds to alternate MESP minima of two oxygens (for example, O_1 and O_7 in Figure 1) in 18C6. EPIC model calculations indeed lead to H_2O molecule binding to these two minima of 18C6, forming two hydrogen bonds as shown in Figure 1. By using this model structure as an initial guess, full ab initio SCF structure is obtained, in which the hydrogen bond distances turn out to be 2.214 and 2.226 Å, respectively (cf. Table 1 with $n = 1$). Table 1 gives the hydrogen bond parameters of the first water molecule (w_1) with 18C6 in the EPIC-model-optimized structure and also in full ab-initio-optimized (HF/6-31G**) complex structures of 18C6·nH_2O ($n = 1$, 2, 3, and 4). In the EPIC model structure of the 18C6·H_2O complex, the distances of the hydrogen bonds formed by hydrogens of water and oxygen of 18C6 are 1.893 and 2.310 Å. The reported parameters in Table 1 show that EPIC-model-optimized geometry indeed serves as a good initial guess for a subsequent full ab initio SCF optimization and the geometrical parameters of hydrogen bonds of first water molecule are not substantially affected on further hydration of 18C6·H_2O.

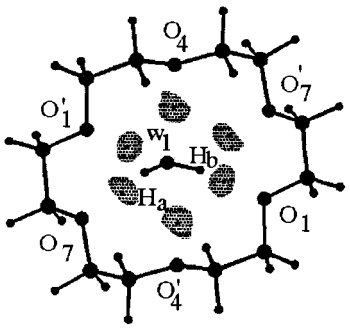

Figure 1. MESP isosurface of value −288.8 kJ mol^{-1} for 18C6 molecule with the enclosed dots denoting minima (−318.9 kJ mol^{-1}). Atom labels according to ref 5. Also shown in EPIC optimized position of water molecule w_1 superposed on this MESP isosurface. See text for details.

TABLE 1: Geometry of Hydrogen Bonds Formed by the First Water Molecule with 18C6, in 18C6·nH_2O ($n = 1$, 2, 3, and 4) Complexes (All Distances, Å; Bond Angles, deg) (See Figure 1 and Text for Details)

18C6·nH_2O params	EPIC[a] model	ab initio SCF[b] $n = 1$	$n = 2$	$n = 3$	$n = 4$
$O_1\cdots H_a(w_1)$	1.893	2.214	2.132	2.119	2.124
$O_7\cdots H_b(w_1)$	2.310	2.226	2.141	2.125	2.128
$O_1\cdots O(w_1)$	2.813	3.101	3.040	3.048	3.052
$O_7\cdots O(w_1)$	3.206	3.107	3.082	3.053	3.056
$O_1\cdots H_a(w_1)-O(w_1)$	164.7	155.7	160.2	166.8	166.3
$O_7\cdots H_b(w_1)-O(w_1)$	158.5	154.7	159.8	166.3	166.1
$O_1\cdots O(w_1)\cdots O_7$	111.3	105.1	106.9	105.1	104.2
$H_a(w_1)-O(w_1)-H_b(w_1)$	106.0	104.2	104.8	105.1	105.3

[a] The parameters in structure optained with the EPIC model. [b] The parameters in full ab initio optimized structure at SCF/6-31G** level.

TABLE 2: Ab Initio HF/6-31G** Energies of 18C6·nH_2O Complexes (All Energies in Atomic Units)

complex	E_{SEP}[a]	E_{SP}(GMAX)[b]	E_{OPT}[c]
18C6·H_2O	−993.535 27	−993.550 95 (0.0105)	−993.554 09
18C6·$2H_2O$	−1069.558 89	−1069.594 85 (0.0126)	−1069.597 57
18C6·$3H_2O$	−1145.582 52	−1145.632 84 (0.0084)	−1145.637 77
18C6·$4H_2O$	−1221.606 14	−1221.678 21 (0.0123)	−1221.680 14
18C6·$6H_2O$[d]	−1373.653 38		−1373.754 15
18C6·$6H_2O$[e]	−1373.653 38		−1373.760 65

[a] E(18C6) = −917.511 66 au and $E(H_2O)$ = −76.023 62 au. These separated energies (E_{SEP}) represent sums: E(18C6) + $nE(H_2O)$. [b] E_{SP}: single point ab initio SCF/6-31G** energy at EPIC model optimized geometry; GMAX, maximum gradient norm of the energy at this geometry. [c] E_{OPT}, full ab initio SCF/6-31G** optimized energy. [d] Structure in Figure 5. [e] Structure in Figure 6.

Table 2 reports the total energies of the 18C6·nH_2O complexes at the HF/6-31G** level. Ab initio HF energies of the complexes of 18C6·nH_2O at single point EPIC model optimized geometries (E_{SP}) differ approximately by 0.01 au from the fully ab initio optimized (E_{OPT}) ones. Table 2 also displays the sum

TABLE 3: Interaction Energies of nH$_2$O (n = 1, 2, 3, and 4) with 18C6 (All Energies in kilojoules per mole)

18C6·nH$_2$O	ΔE_{EPIC}^{STEP}[a]	ΔE_{OPT}^{STEP}[b]	ΔE_{EPIC}^{TOTAL}[c]	ΔE_{SCF}^{TOTAL}[d]
1. 18C6·H$_2$O	40.97	49.40	40.97	49.40
2. 18C6·2H$_2$O	43.01	52.16	83.98	101.56
3. 18C6·3H$_2$O	40.07	43.54	124.05	145.10
4. 18C6·4H$_2$O	43.71	49.25	167.76	194.35

[a] ΔE_{EPIC}^{STEP}: Stepwise interaction of H$_2$O with 18C6·nH$_2$O (n = 0, 1,2, 3,). [b] ΔE_{OPT}^{STEP}: Full optimized *ab initio* SCF/6-31G** interaction energy, defined as $\Delta E_{OPT}^{STEP} = E_{OPT}$(18C6·$nH_2$O) − [($E_{OPT}$(18C6·($n$ − 1)H$_2$O) + E_{OPT}(H$_2$O)], where E_{OPT} is the same as above defined in Table 2. [c] ΔE_{EPIC}^{TOTAL}: Total binding energy of 18C6 with nH$_2$O with the EPIC model. [d] ΔE_{SCF}^{TOTAL}: Total interaction energy of 18C6 with nH$_2$O with full *ab initio* SCF/6-31G** level calculation, defined as $\Delta E_{SCF}^{TOTAL} = E_{OPT}$(18C6-$nH_2$O) − [$E_{OPT}$(18C6) + nE(H$_2$O)], where E_{OPT} is the same as above defined in Table 2.

of separated energies (E_{SEP}) defined as $E_{SEP} = E$(18C6) + nE(H$_2$O) where E(18C6) and E(H$_2$O) are ab initio SCF energies of fully optimized 18C6 and H$_2$O molecules, respectively. A comparison of these separated energies, viz., E_{SEP}, with the energies E_{SP} and E_{OPT}, brings out the substantial binding of a single additional H$_2$O molecule with 18C6·nH$_2$O (n = 0, 1, 2, 3), with the interaction energies in the range of 43−52 kJ mol^{-1} (see also Table 3). It may also be noticed that the single point HF/6-31G** energies in the second column of Table 2 approximate quite well the corresponding fully optimized ones. Further, the maximum gradient norms reported in Table 2 are all in the range of 0.01 au, indicating that the starting geometries are indeed reasonably good. Table 3 lists the stepwise model interaction energies (ΔE_{EPIC}^{STEP}) of H$_2$O with fully ab initio optimized 18C6·nH$_2$O (n = 0, 1, 2, 3) moieties. These model interaction energies show trends similar to stepwise fully ab initio optimized interaction energies ΔE_{OPT}^{STEP} of H$_2$O with 18C6·nH$_2$O, defined as

$$\Delta E_{OPT}^{STEP} = E_{OPT}(18C6.nH_2O) - [E_{OPT}(18C6\cdot(n-1)H_2O) + E_{OPT}(H_2O)]$$

The total (cumulative) interaction energies of 18C6·nH$_2$O obtained with EPIC model (ΔE_{EPIC}^{TOTAL}) as well as with full ab initio SCF (ΔE_{SCF}^{TOTAL}) computations are also shown in Table 3. These ΔE_{EPIC}^{TOTAL} interaction energies are in the range of 83−86% of the corresponding ΔE_{SCF}^{TOTAL} ones, which shows that the EPIC model yields not only reasonably good geometrical parameters but also faithfully brings out trends in interaction energies.

Having examined the energetics of crown ether hydration, we now focus on the driving force for this, viz., the cooperative electrostatics effects. The topographical analysis of 18C6·H$_2$O brings out that the values of MESP minima of w$_1$ (−386.0 and −370.2 kJ mol^{-1}) become much deeper than the values (each of −261.2 kJ mol^{-1}) of the MESP minima of an individual water molecule. This creates a lock-and-key arrangement with the second (w$_2$) incoming water molecule acting as the key. From the negative-valued MESP isosurfaces (−354.4 (dark) and −262.6 (light) kJ mol^{-1}) of 18C6·H$_2$O complex in Figure 2, one can predict that the second water molecule (w$_2$) will form two hydrogen bonds. One is expected to be formed with the oxygen MESP minimum of the first water molecule and another with the MESP minimum of O$_4$ (cf. Figure 1) of 18C6. The O$_4$ atom on the face of 18C6, where the first water molecule is bound, is endowed with the deepest MESP minimum among the oxygen minima of 18C6 in the 18C6·H$_2$O complex. Figure 2 also depicts the EPIC-model-optimized position of the second water molecule, forming the above-mentioned two hydrogen bonds with the 18C6·H$_2$O complex. The total interaction energy within EPIC model, viz, ΔE_{EPIC}^{TOTAL}, of 18C6·2H$_2$O turns out to be 83.98 kJ mol^{-1}, whereas the total ab initio interaction energy ΔE_{SCF}^{TOTAL} of the same after full optimization is 101.56 kJ mol^{-1}.

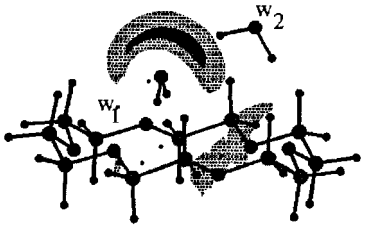

Figure 2. Two MESP isosurfaces [−354.4 (dark) and −262.6 (light) kJ mol^{-1}] for 18C6·H$_2$O upon which is superposed the EPIC optimized position of w$_2$. See text for details.

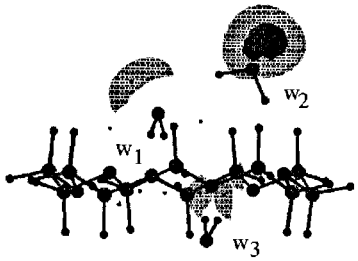

Figure 3. Two MESP isosurfaces [−341.3 (dark) and −241.6 (light) kJ mol^{-1}] for 18C6·2H$_2$O. Also superposed is EPIC optimized position of w$_3$. More details are given in text.

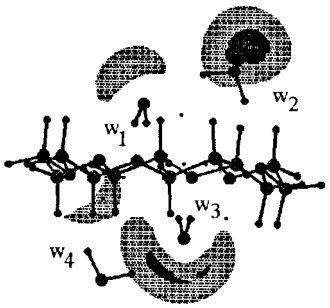

Figure 4. Two MESP isosurfaces [−325.6 (dark) and −196.9 (light) kJ mol^{-1}] for 18C6·3H$_2$O. EPIC optimized position of w$_4$ is superposed. More details are given in text.

Figure 3 shows the mapped MESP isosurfaces of values −341.3 (dark) and −241.6 (light) kJ mol^{-1} of 18C6·2H$_2$O at full ab initio SCF-optimized structure. The values of MESP minima of second water molecule are −379.0 and −377.8 kJ mol^{-1}. Due to this, one may expect the third water molecule (w$_3$) to bind to the oxygen of w$_2$. However, with this arrangement, it will form only a single hydrogen bond because crown ether oxygens are blocked by w$_1$ and w$_2$. On the other hand, three MESP minima of three oxygens (O$_1'$, O$_4'$, and O$_7'$) of 18C6 are still available on the other face of 18C6. Out of these three, two are quite deep (cf. Figure 3), where the third water molecule (w$_3$) may bind rather similarly to the first water molecule (w$_1$). Figure 3 also includes the EPIC-model-optimization position of the third water with the fully optimized 18C6·2H$_2$O. The rank order of interaction energies reported in Table 3 can thus be rationalized.

Figure 4 depicts two MESP isosurfaces of values −325.6 (dark) and −196.9 (light) kJ mol^{-1}, respectively, evaluated at the full ab initio HF optimized structure of 18C6·3H$_2$O. From

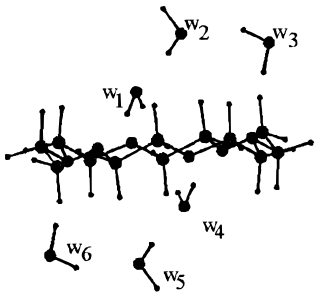

Figure 5. Ball-and-stick model of ab initio optimized geometry of 18C6·6H_2O complex, denoted as (d) in Table 2. See text for further details.

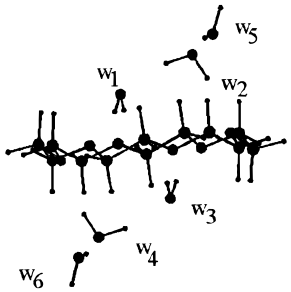

Figure 6. Ball-and-stick model of another ab initio optimized geometry of 18C6·6H_2O complex, denoted as (e) in Table 2. See text for further details.

these MESP isosurfaces, one may predict the fourth incoming water molecule (w_4) to bind by forming two hydrogen bonds with the oxygen minima of w_3 and the crown ether, showing a beautiful complementary arrangement. Total and stepwise EPIC-model interaction energies and fully ab initio optimized energies reported in Table 3 for the 18C6·4H_2O complex are also qualitatively similar. Thus, the utility of the EPIC model for the preliminary purpose of predicting patterns in hydration energies and geometries of the crown ether hydration problem is brought out by the study of 18C6·$n$$H_2O$ ($n = 1-4$).

Yet another attractive feature of the EPIC model is that one may use the block diagonal density matrix for 18C6·$n$$H_2O$ obtained by patching the corresponding individual density matrices of 18C6·($n - 1$)H_2O and H_2O. This enables one to avoid a full ab initio HF calculation of the density matrix for 18C6·$n$$H_2O$ in order to study further hydration. With this method, the total interaction energy obtained by the EPIC model of 18C6 with four water molecules in 18C6·4H_2O turns out to be 168.49 kJ mol^{-1}. The total interaction energy of the same complex with the EPIC model in which full ab initio optimized density matrices of 18C6·($n - 1$)H_2O and H_2O are progressively used yields a quite similar value, viz., 167.76 kJ mol^{-1}.

Figures 5 and 6 show two complex structures of 18C6·6H_2O obtained with the EPIC model, in which patched density matrices are progressively used (as discussed in the above paragraph). The total interaction energy obtained with the EPIC model is 232.26 kJ mol^{-1} of the structure in Figure 5. After full optimization at the ab initio HF level, the total interaction energy yields 264.57 kJ mol^{-1} of 18C6 with six H_2O molecules. Figure 6 depicts yet another structure of the 18C6·6H_2O complex, which is also obtained in a similar way, with the ab initio HF total interaction energy of 281.63 kJ mol^{-1}. Thus, this structure is more stable than the one shown in Figure 5 by 17.06 kJ mol^{-1}. The total ab initio HF/6-31G** energies are reported in Table 2. Detailed optimized geometries of 18C6·$n$$H_2O$ are available from the authors upon request. Carrying on this exercise further, one may predict further hydrated structures of 18C6, e.g. 18C6·8H_2O, 18C6·12H_2O, etc. This work is in progress in our laboratory.

Concluding Remarks

The problem of hydration of molecules and ions has been actively pursued along two active lines of research in the literature, as pointed out in the Introduction. One of the methods is ab initio quantum chemical treatment with the other one being computer simulations/dynamics/modeling studies. Both of these methods do not provide a direct molecular level picture of the stepwise hydration process, including the *how and why of it*. Other models popular in the chemical literature also do not provide such a picture. The topographical feature of MESP coupled with the energetic aspects described by the MESP model thus seem to offer an invaluable tool for exploring hydration processes. A useful pictorial representation of the strength of interaction involved is offered by the MESP topography, and isosurface as brought out in Figures 1−4. A qualitative and semiquantitative understanding of why the second water molecule binds more strongly than the first is apparent from the MESP features of 18C6 and 18C6·H_2O in Figures 1 and 2. Thus the answer to the question posed by Ranghino et al.[16] quoted in the Introduction now seems to be in the affirmative. It is thus indeed possible to obtain valuable insights into the hydration processes of molecules (including ions) with the present approach in a rather simple way. In fact, the present approach is readily applicable to other solvent molecules (e.g. methanol, chloroform, etc.) as well. From the correlation between the model interaction energies and SCF HF/6-31G** ones, it seems that polarization effects are not very large in hydration processes of neutral molecules, but their inclusion may further improve the quantitative value of the present approach, as pointed out in ref 12. The hydration process for a few interesting molecular species, including cations and anions, with a variety of solvents is currently being investigated in our research group wherein the polarization effect is also incorporated.

Acknowledgment. Support from the Council of Scientific Research New Delhi [Grants 1(1430)/96-EMR-II) and 9/137(286)/96-EMR-I] is gratefully acknowledged by S.R.G. and S.S.P., respectively. The authors thank Professor K. J. Patil for bringing the crown ether hydration problems to our attention.

References and Notes

(1) See, for a collections of articles on this subject: Smith, D. A., Ed. *Modeling the Hydrogen Bond*; American Chemical Society: Washington, D.C., 1994; in particular, the articles by Gao, J. (pp 8−21) and Keith, T. A.; Frisch, M. J. (pp 22−35).

(2) For a lucid comprehensive treatment, see: Jeffrey G. A. *An Introduction to Hydrogen Bonding*; Oxford University Press: New York, 1997.

(3) See, for example: Mootz, D.; Wussow, H.-G. *J. Chem. Phys.* **1981**, *74*, 1517−1522.

(4) Mootz, D.; Schilling, M. *J. Am. Chem. Soc*. **1992**, *114*, 7435−7439.

(5) Zhanpeisov, N. U.; Leszczynski, J. *Int. J. Quantum Chem*., in press.

(6) Gorb, L.; Leszczynski, J. *J. Am. Chem. Soc*., in press.

(7) Šponer, J.; Leszczynski, J.; Vetter, V.; Hobza, P. *J. Biomol. Struct. Dyn*. **1996**, *13*, 695.

(8) Šponer, J.; Leszczynski, J.; Hobza, P. *J. Phys. Chem*. **1998**, *100*, 5590.

(9) (a) de Olivera, M. *J. Comput. Chem*. **1986**, *7*, 617−628. (b) de Olivera, M. *J. Comput. Chem.* **1986**, *7*, 629−639.

(10) (a) Orozco, M.; Luque, F. J. *J. Comput. Chem*. **1993**, *14*, 587−602. (b) Orozco, M.; Luque, F. J. *Biopolymers* **1993**, *33*, 1851.

(11) Alhambra, C.; Luque, F. J.; Orozco, M. *J. Phys. Chem*. **1995**, *99*, 3084−3092.

(12) (a) Luque, F. J.; Orozco. M. *J. Comput. Chem.* **1998**, *19*, 866−881. (b) Orozco, M.; Luque, F. J.; Habibollahzadeh, D.; Gao, J. *J. Chem. Phys.* **1995**, *189*, 6145−6152.

(13) (a) Patil, K. J.; Heil, S. R.; Holz, M.; Zeidler, M. D. *Ber. Bunsen-Ges.. Phys. Chem.* **1997**, *101*, 91−95. (b) Patil, K. J.; Pawar, R. Unpublished work.

(14) Mootz, D.; Albert, A.; Schaefgen, S.; Staben, D. *J. Am. Chem. Soc*. **1994**, *116*, 12045−12046.

(15) Albert, A.; Mootz, D. *Z. Naturforsch*. **1997**, *52b*, 615−619.

(16) Ranghino, G.; Romano, S.; Lehn, J. M.; Wipff, G. *J. Am. Chem. Soc.* **1985**, *107*, 7873−7877.

(17) (a) Fukuhara, K.; Tachikake, M.; Matsumoto, S.; Matsuura, H. *J. Phys. Chem.* **1995**, *99*, 8617−8623. (b) Matsuura, H.; Fukuhara, K.; Ikeda, K.; Tichikake, M. *J. Chem. Soc., Chem. Commun.* **1989**, 1814−1816. (c) Takeuchi, H.; Arai, J.; Harada, I. *J. Mol. Struct.* **1986**, *146*, 197−212. (d) Fukushima, K.; Ito, M.; Sakurada, K.; Shieaishi, S. *Chem. Lett*. **1988**, 323−326. (e) Miyazawa, M.; Fukushima, K.; Oe, S. *J. Mol. Struct*. **1989**, *195*, 271−281. (f) Zhelyaskov, V.; Georgiev, G.; Nicholov, Zh.; Miteva, M. *Spectrochim. Acta, Part A* **1989**, *45*, 625−633. (g) Ozutsumi, K.; Natsuhara, M.; Ohtaki, H. *Bull. Chem. Soc. Jpn.* **1989**, *62*, 2807−2818. (h) Georgiev, G.; Nickolov, J.; Nickolov, Zh.; Zhelyaskov, V. *Spectrochim. Acta, Part A* **1991**, *47*, 749−757. (i) Fukuhara, K.; Ikeda, K.; Matsuura, H. *Spectrochim. Acta, Part A* **1994**, *50*, 1619−1628, and references cited therein.

(18) Kowall, T.; Geiger, A. *J. Phys. Chem*. **1994**, *98*, 6216−6224.

(19) Bryan, S. A.; Willis, R. R.; Moyer, B. A. *J. Phys. Chem*. **1990**, *94*, 5230−5233.

(20) Pelc, H. W.; Hempelmann, R.; Prager, M. Zeidler, M. D. *Ber. Bunsen-Ges. Phys. Chem*. **1991**, *95*, 592−598.

(21) (a) Liesegang, G. W.; Farrow, M. M.; Purduie, N. Eyring, E. M. *J. Am. Chem. Soc.* **1976,** *98*, 6905−6908. (b) Chen, C. C.; Petrucci, S. *J. Phys. Chem.* **1982**, *86*, 2601−2605. (c) Miynard, K. J.; Irish, D. E.; Eyring, E. M.; Petrcci, S. *J. Phys. Chem*. **1984**, *88*, 729−736. (d) Rodriguez, L. J.; Eyring, E. M.; Petrucci, S. *J. Phys. Chem.* **1989**, *93*, 6357−6363. (e) Miyazaki, Y.; Matsuura, H. *Bull. Chem. Soc. Jpn.* **1991**, *64*, 288−290. (f) Firman, P.; Rodriguez, L. J.; Petrucci, S.; Eyring, E. M. *J. Phys. Chem*. **1992**, *96*, 2376−2381.

(22) (a) Wipff, G.; Weinder, P.; Kollman, P. *J. Am. Chem. Soc*. **1982**, *104*, 3249−3258. (b) Uiterwijk, J. W. H. M.; Harkema, S.; Feil, D. *J. Chem. Soc., Perkin Trans. 2* **1987**, 721−731.

(23) (a) van Eerden, J.; Harkema, S.; Feil, D. *J. Phys. Chem*. **1988**, *92*, 5076−5079. (b) Straatsma, T. P.; McCommon, J. A. *J. Chem. Phys*. **1989**, *91*, 3631−3637. (c) van Eerden, J.; Briels, W. J.; Harkema, S.; Feil, D. *Chem. Phys. Lett.* **1989**, *164*, 370−376. (d) Mazor, M. H.; McCommon, J. A.; Lybrand, T. P. *J. Am. Chem. Soc.* **1989**, *111*, 55−56. (e) Dang, L. X.; Kollman, P. A. *J. Am.* Chem. *Soc.* **1990**, *112*, 5716−5720. (f) Sun, Y.; Kollman, P. A. *J. Am. Chem. Soc.* **1992**, *97*, 5108−5112. (g) Kowall, T.; Geiger, A. *J. Phys. Chem*. **1994**, *98*, 6216−6224.

(24) Ha, Y. L.; Chakraborty, A. K. *J. Phys. Chem*. **1991**, *95*, 10781−10787.

(25) (a) Bonaccorsi, R.; Scrocco, E.; Tomasi, J. *J. Chem. Phys*. **1970**, *52*, 5270. Scrocco, E.; Tomasi, J. *Topics in Current Chemistry*; Springer: Berlin, 1973; Vol. 42. (b) Scrocco, E.; Tomasi, J. *Adv. Quantum Chem.* **1978**, *11*, 115.

(26) (a) Politzer, P.; Daiker, K. C. *Chem. Phys. Lett.* **1975**, *34*, 294. (b) Politzer, P.; Murray, J. S. In *Structure and Reactivity*; Liebman, J. F., Greenberg, A., Eds.; VCH: Weinheim, Germany, 1988; Chapter 1.

(27) (a) Orita, Y.; Pullman, A. *Theor. Chim. Acta* **1977**, *46*, 251. (b) Orita, Y.; Pullman, A. *Theor. Chim. Acta* **1977**, *45*, 257. (c) Kearney, P. C.; Mizoue, L. S.; Kumpf, R. A.; Forman, J. E.; McCurdy, A.; Dougherty, D. A. *J. Am. Chem. Soc*. **1993**, *115*, 9907. (d) Kumpf, R. A.; Dougherty, D. A. *Science* **1993**, *261*, 1708. (e) Dougherty, D. A. *Science* **1996**, *271*, 163. (f) Mecozzi, S.; West, A. P., Jr.; Dougherty, D. A. *J. Am. Chem. Soc.* **1996**, *118*, 2307. (g) Mecozzi, S.; West, A. P., Jr.; Dougherty, D. A. *Proc. Natl. Acad.* Sci. U.S.A. **1996**, *93*, 10566.

(28) (a) Caldwell, J. W.; Kollman, P. A. *J. Am. Chem. Soc.* **1995**, *117*, 4177. (b) Cerda, B. A.; Wesdemiotis, C. *J. Am. Chem. Soc.* **1996**, *118*, 11884.

(29) Goldfuss, B.; Schleyer, P. v. R.; Hampel, F. *J. Am. Chem. Soc*. **1996**, *118*, 12183.

(30) Murray, J. S.; Sen, K. *Molecular Electrostatic Potentials: Concepts and Applications Edition;* Elsevier: Amsterdam, **1996.** In particular, see the following articles in this monograph: (a) Tomasi, J.; Mennucci, B.; Cammi, R. p 1. (b) Orozco, M.; Luque, F. J. p 181. (c) Gadre, S. R.; Bhadane, P. K.; Pundlik, S. S.; Pingale, S. S. pp 219−255. (d) Mishra, P. C.; Kumar, A. p 257. (e) Náray-Szabó, G. p 333. (f) Alcamí, M.; Mö, O.; Yáñez, M. p 407.

(31) (a) Stöckigt, D. J. *Phys. Chem. A* **1997**, *101*, 3800. (b) Ma, J. C.; Dougherty, D. A. *Chem. Rev*. **1997**, *97*, 1303.

(32) Frisch, M. J.; Trucks, G. W.; Schlegel, H. B.; Gill, P. M. W.; Johnson, B. G.; Robb, M. A.; Cheeseman, J. R.; Keith, T.; Petersson, G. A.; Montgomery, J. A.; Raghavachari, K.; Al-Laham, M. A.; Zakrzewski, V. G.; Ortiz, J. V.; Foresman, J. B.; Cioslowski, J.; Stefanov, B. B.; Nanayakkara, A.; Challacombe, M.; Peng, C. Y.; Ayala, P. Y.; Chen, W.; Wong, M. W.; Andres, J. L.; Replogle, E. S.; Gomperts, R.; Martin, R. L.; Fox, D. J.; Binkley, J. S.; Defrees, D. J.; Baker, J.; Stewart, J. P.; Head-Gordon, M.; Gonzalez, C.; Pople, J. A. *GAUSSIAN 94*; GAUSSIAN, Inc.: Pittsburgh, PA, 1995.

(33) Adequacy of basis set: Expansion of basis set beyond[33a,b] 6-31G** level as well as incorporating electron correlation does not generally result in significant change in the MESP topography. This basis set is known to be adequate[31b] for investigating weak complexes. See: (a) Kulkarni, S. A. *Chem. Phys. Lett.* **1996**, *254*, 268. (b) Gadre, S. R.; Kulkarni, S. A.; Suresh, C. H.; Shrivastava, I. H. *Chem. Phys. Lett*. **1995**, *239*, 273.

(34) (a) Gadre, S. R.; Shrivastava, I. H. *J. Chem. Phys.* **1991**, *94*, 4384. (b) Gadre, S. R.; Kulkarni, S. A.; Shrivastava, I. H. *J. Chem. Phys*. **1992**, *96*, 5253.

(35) (a) Stewart, I. *Sci. Am.* **1991**, *364*, 123. (b) Bader, R. F. W.; Nguyen-Dang, T. T.; Tal, Y. A. *Rep. Phys*. **1981**, *44*, 893.

(36) The package INDPROP developed by Gadre et al.; see: Shirsat, R. N.; Bapat, S. V.; Gadre, S. R. *Chem. Phys. Lett.* **1992**, *200*, 373−378.

(37) The FORTRAN program GRID, performing charge fitting to molecular electrostatic potentials available from: Chipot, C. University De Nancy I, France. We are thankful to Dr. C. Chipot for supplying us this code. See also: Chipot, C.; Ángyán, J. G.; Ferenczy, G. G.; Scheraga, H. A. *J. Phys. Chem*. **1993**, *97*, 6628−6636.

(38) Pauling, L. *The Nature of the Chemical Bond*; Cornell University Press: Ithaca, NY, 1942.

(39) Gadre, S. R.; Bhadane, P. K. *J. Chem. Phys.* **1997**, *107*, 5625.

(40) A Fortran code UNIVIS developed at the University of Pune: see Limaye, A. C.; Inamdar, P. V.; Dattawadkar, S. M.; Gadre, S. R. *J. Mol. Graph*ics **1996**, 14−19.